Tin sulfide-based nanocomposite: synthesis and study of structural, morphological and optical properties

G. Murugadoss[a,*], M. R. Kumar[b,*], A. Kathalingam[c], R. Jothiramalingam[d#], H. Al-Lohedan[d], D. M. Al-Dhayan[d]

[a]*Centre for Nanoscience and Nanotechnology, Sathyabama Institute of Science and Technology, Chennai 600119, Tamil Nadu, India*

[b]*Institute of Natural Science and Mathematics, Ural Federal University, Yekaterinburg 620002, Russia*

[c]*Millimeter-wave Innovation Technology Research Center, Dongguk University-Seoul, Seoul 04620, Republic of Korea*

[d]*Department of chemistry, College of science, King Saud University, PO Box 2455, Riyadh 11451, Kingdom of Saudi Arabia*

A facile one-step chemical method has been developed for synthesize of SnS-based nanocomposites. Herein, we have prepared a series of SnS based nanocomposites such as SnS/CdO, CdO/SnS, SnS/PbO, PbO/SnS, SnS/PbS and PbS/SnS. The synthesized nanocomposites were characterized using X-ray diffraction (XRD), transmission electron microscope (TEM), Fourier transform infrared (FT-IR), UV-visible and Photoluminescence (PL) spectroscopy. The obtained results are discussed in details. Significant PL sifting observed for SnS based nanocomposites. The role of the various compounds added with SnS is mainly for tunning the optical emission of the SnS. The obtained visible light emission of the SnS-based nanocomposites can be used in the optoelectronic applications.

(Received October 7, 2021; Accepted February 1, 2022)

Keywords: chemical method, Nanocomposites, TEM, Band gap, Photoluminescence

1. Introduction

Doped semiconductors are the most important building elements for modern electronic devices [1]. Tin sulfide (SnS) is IV-VI binary semiconductor compound, their constituent elements Sn and S are abundant and are less toxic in nature. SnS has p-type conductivity, orthorhombic structure with both direct and indirect band gap values 1.3–1.5 eV and 1.0–1.1 eV, respectively. Tin sulfide has variety of applications in optoelectronic devices, biotechnology and biomedicines etc [9-11]. Composite formation seems to be an effective strategy which could improve the physical properties of SnS [14]. Cadmium oxide (CdO) is a II-VI group transition metal oxide semiconductor which seems to be very photoactive due to its narrow band gap. Due to its favourable visible light absorption and high charge carrier mobility CdO seems to be an efficient photocatalyst for dye degradation [15]. Enhanced photocatalytic and photoelectrochemical properties have been reported for TiO_2 nanoparticles when coupled with CdO [16, 17]. Lead oxide (PbO), is another important industrial material due to its unique electronic, mechanical and optical properties and its potential applications in nano devices and functionalized materials [18]. Because of the simplicity of design, low cost of manufacturing, reliability and relative safety there is improve and develop lead oxide characteristics. PbS is also an important IV–VI semiconductor material with rather small band gap (0.41 eV at 300 K) [19] and relatively large excitation Bohr radius (18 nm) [20]. PbS band gap can be widened to the visible region by forming nanocrystals.

Herein we have synthesized SnS-based nanocomposite with modified CdO, PbO, and PbS and investigated their structural, morphological and optical properties.

* Corresponding author: jrajabathar@ksu.edu.sa
https://doi.org/10.15251/JOR.2022.181.67

2. Experimental details

2.1. Materials

Tin (II) chloride dihydrate ($SnCl_2$•$2H_2O$), Lead (II) acetate trihydrate $(CH_3COO)_2Pb$•$3H_2O$, Cadmium acetate dihydrate $(CH_3COO)_2Cd$•$2H_2O$, Sodium sulfide ($N_2S.xH_2O$) and sodium hydroxide were purchased from sigma Aldrich. All the chemical were used in high purity in AR grade. The solvent such ethanol and acetone were purchased from Loba chemical Pvt. Ltd. Ethanol was used as solvent for whole synthesize procedure.

2.2. Synthesis of Tin Sulfide-based nanocomposites

The Sn-based nanocomposites were synthesized using a facile chemical precipitation method. Typically, 0.2 M of $SnCl_2$•$2H_2O$ was dissolved in 50 ml of ethanol under stirring at 80°C. Then, 0.5 g of polyvinylpyrrodine (PVP) was added to the above solution. After dissolved the above precursor, 0.2 M of Na_2S in 50 ml was added to the above solution under stirring. After 1h, second metal precursor was added to the above solution for preparation of the nanocomposite. Finally, Na_2S or NaOH was added to the above solution based on the required composites. After the reaction was completed, the solution was cooled down to room temperature. Then, the colloidal solution was washed with ethanol and acetone for several times. Subsequently, the prepared product was dried at 120 °C for 12 h and then the resultant products were used for further characterization.

2.3. Characterization

The crystal structural of the synthesized nanocomposites were examined by X-ray diffraction (XRD) pattern using an X'pert PRO diffractometer with CuKα radiation (λ = 1.54060Å) at room temperature. The morphology and particles size of the nanocomposites were obtained from TEM (Technai20G2, FEI) microscopy. The functional groups on the surface of nanocomposite were examined by FT-IR (BRUKER-TENSOR 27) spectrometer using KBr pellets. The optical the nanocomposites were studied using a UV-1650PC SHIMADZU Spectrophotometer. Fluorescence measurements were performed on a RF-5301PC Spectrophotometer.

3. Results and Discussion

The crystalline phases and structures of the as-synthesized Tin sulfide-based nanocomposites were confirmed via X-ray diffraction (XRD) spectrometer as shown in Fig. 1(a-c). Fig. 1 shows X-ray diffraction patterns of (a) SnS/CdO and CdO/SnS, (b) SnS/PbO and PbO/SnS, and (c) SnS/PbS and PbS/SnS nanocomposites. From Fig. 1(a-c), all the diffractions are well matched with orthorhombic SnS (Space group: Pbnm, JCPDS No. 39-0354) and cubic CdO (JCPDS No. 05-0640), similarly, orthorhombic structure of PbO (JCPDS No. 38-1477) and cubic of PbS (JCPDS No. 78-1057) as shown in the diffraction pattern of Fig. 1(b). The Fig. 1(c) shows XRD pattern of SnS/PbS and PbS/SnS nanocomposites, all the diffractions are well matched with orthorhombic (SnS) and cubic (PbS) structure. The crystalline size of nanocomposites was calculated using Scherrer formula,

$$D = (0.9\lambda) / (\beta \cos\theta) \quad (1)$$

where λ is the wavelength of X-ray radiation, β is the full width at half maximum (FWHM) of the peaks at the diffracting angle θ. The average sizes of SnS/CdO, CdO/SnS, SnS/PbO, PbO/SnS, SnS/PbS and PbS/SnS nanocomposites were found to be 18-28 nm range. The strong diffraction peaks and absence of the impurity peaks are clearly demonstrated the synthesized chemical method offered high quality of the SnS-based nanocomposites.

TEM microscopy gives actual information about size and structure of the composites. The TEM images with different magnification of SnS/CdO (Fig. 2a-d)), SnS/PbO (Fig. 3a-d) and SnS/PbS (Fig. 4a-d) nanocomposites and corresponding SAED patterns were measured for the

powder samples. Fig. 2(a-c) shows the morphology of SnS/CdO nanocomposites (different magnifications), it clearly shows the formation of SnS/CdO nanocomposites with both cubic and orthorhombic structures. Fig. 3(a-c) shows the sample (SnS/PbO) contains small grains agglomerated with the spherical shape. A uniform grain size of both SnS and PbO were observed, which gives supporting evidence for the homogeneous mixing of both SnS and PbO. Fig. 4(a-c) the TEM images of SnS/PbS nanocomposites, shows a rod-like structure mixed with the triangular shape of aggregated particles. Figures (Figs. 2d, 3d, 4d) show the corresponding selected-area electron diffraction (SAED) patterns of SnS/CdO, SnS/PbO and SnS/PbS nanocomposites, respectively. The clear spots on the circle show well crystalline nature of the nanocomposite.

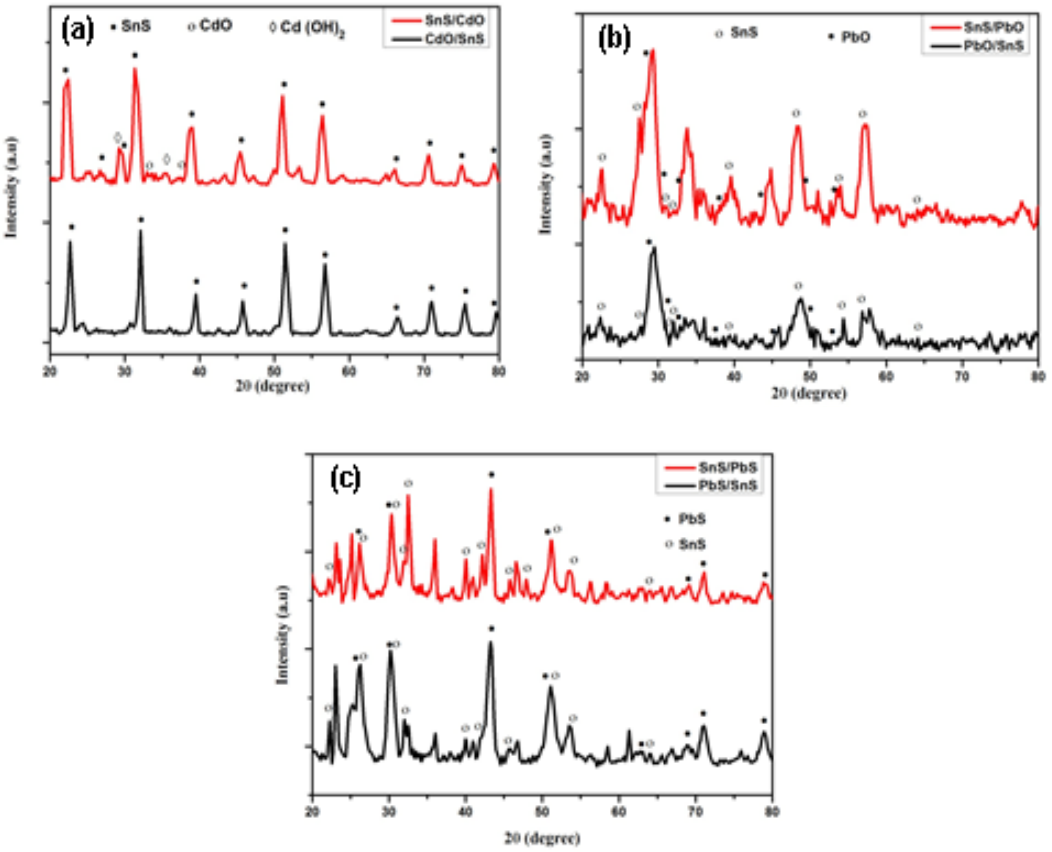

Fig. 1. X-ray diffraction spectra of (a) SnS/CdO and CdO/SnS (b) SnS/PbO and PbO/SnS (c) SnS/PbS and PbS/SnS nanocomposites. The characteristic peaks of the corresponding samples are marked with different asterisks.

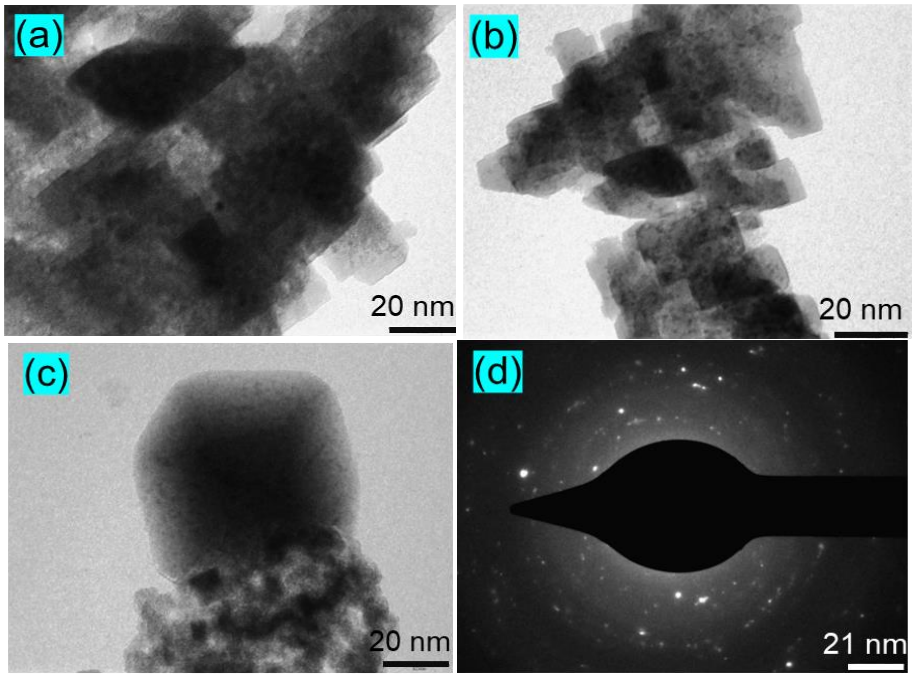

Fig. 2 (a-c) TEM images of SnS/CdO nanocomposites with different magnifications (d) corresponding selected-area electron diffraction (SAED) pattern.

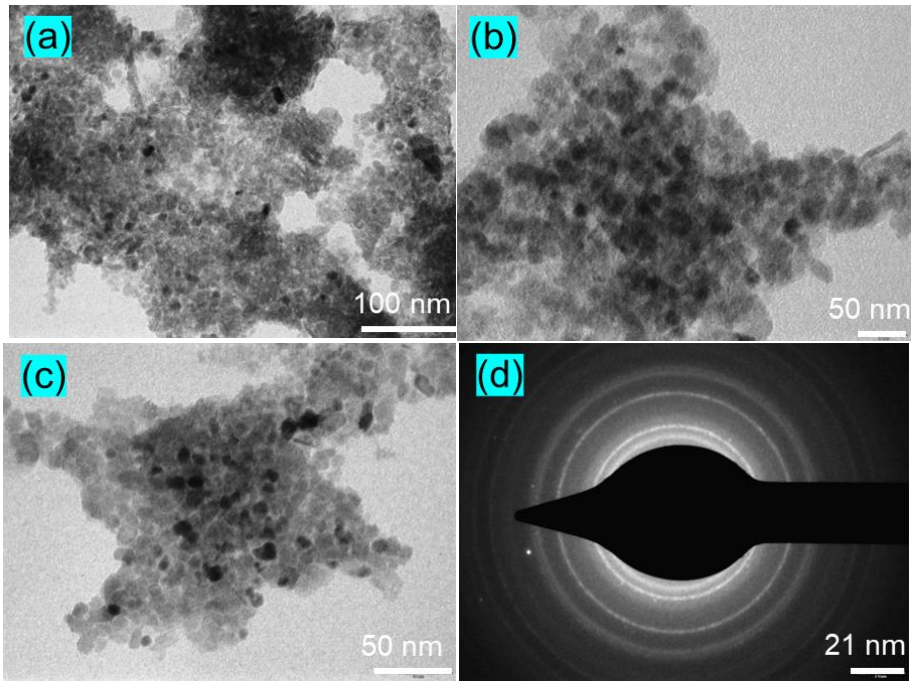

Fig. 3. (a-c) TEM images of SnS/PbO nanocomposites with different magnifications (d) corresponding selected-area electron diffraction (SAED) pattern.

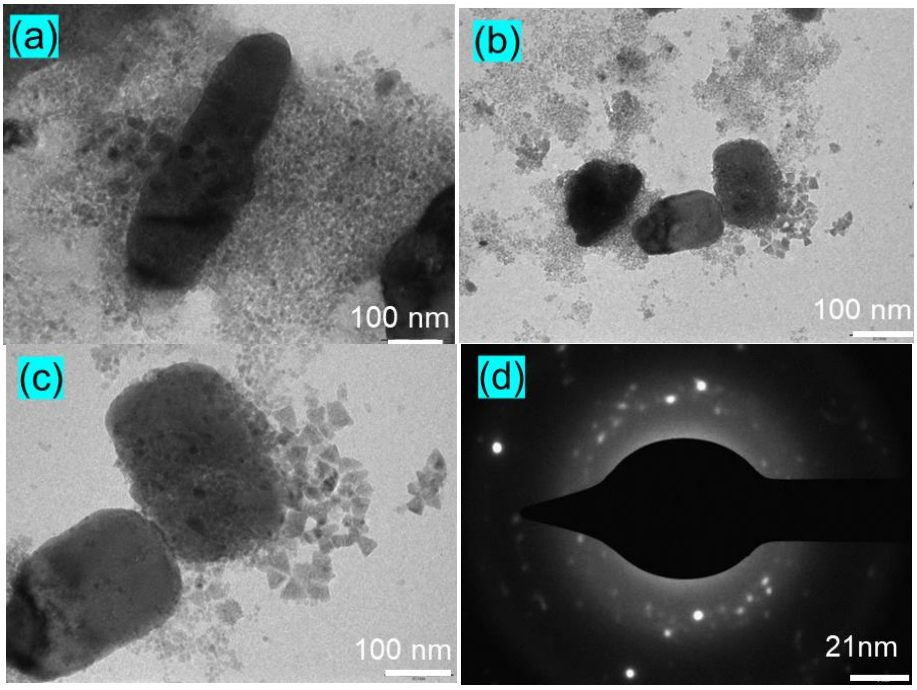

Fig. 4 (a-c) TEM images of SnS/PbS nanocomposites with different magnifications (Scale bar 20 nm) (d) corresponding selected-area electron diffraction (SAED) pattern.

FT-IR spectrum of SnS/CdO, CdO/SnS, SnS/PbO, PbO/SnS, SnS/PbS and PbS/SnS nanocomposites are shown in Fig. 5. For all nanocomposites, the peaks at 647, 1000-1200, 1371, 1460 cm^{-1} and broad valley at 750-950 cm^{-1} correspond to SnS and the absorption at 2350 cm^{-1} for hydroxyl group. Besides the SnS vibrations, a significant broad absorption peak at 3200-3550 cm^{-1}, is due to the strong OH stretching vibrations. In particular, the broad OH stretching vibrations exists more in SnS/CdO and CdO/SnS nanocomposites may be due to the presence of $Cd(OH)_2$ impurity as observed in XRD results. The weak band near 1625 cm^{-1} is assigned to H–O–H bending vibrations mode probably due to the water adsorption at the time of sample preparation.

The UV–vis absorption spectra of SnS/CdO, CdO/SnS, SnS/PbO, PbO/SnS, SnS/PbS and PbS/SnS nanocomposites are shown in Figure 6(a). UV-Vis absorption spectra of all nanocomposites such as SnS/CdO, CdO/SnS, SnS/PbO, PbO/SnS, SnS/PbS and PbS/SnS display strong absorption in the near visible region, indicating that samples possesses high utilization efficiency for natural sunlight. The samples show absorption peaks at around 551 nm, 327 nm, 459 nm, 335 nm, 365 nm and 344 nm for SnS/CdO, CdO/SnS, SnS/PbO, PbO/SnS, SnS/PbS and PbS/SnS nanocomposites, respectively. The peak differences for SnS/metal oxide and metal oxide/SnS are significantly higher about 100 nm than SnS/metal sulfide and metal sulfide/SnS. The shifting of the absorption is may due to quantum confinement effect on the particle size.

Band gap was determined by Tauc plot from the formula of $\alpha h\nu = A(h\nu - E_g)^{1/2}$, where α is the material optical absorbance, hν is the photon energy, E_g is bandgap energy value. Tauc plot was delineated in Figure 6(b) with the optical bandgaps of SnS/CdO, CdO/SnS, SnS/PbO, PbO/SnS, SnS/PbS and PbS/SnS nanocomposites which were respectively calculated to be 2.2, 3.8, 2.7, 3.7, 3.4 and 3.6 eV. It is clear that there is huge bandgap difference for Tin sulfide/metal oxide and metal oxide/Tin sulfide nanocomposites (~1 eV) whereas band gap difference between Tin sulfide/metal sulfide and metal sulfide/Tin sulfide nanocomposites are very small (~0.2 eV).

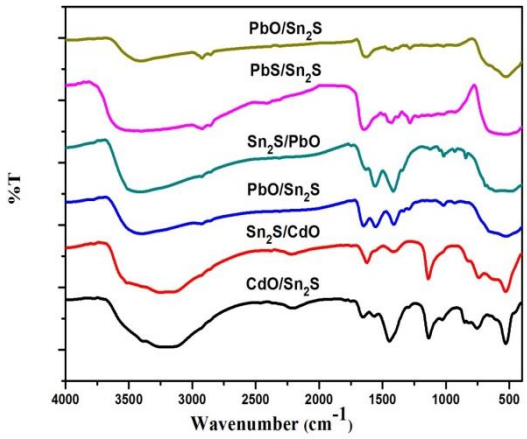

Fig. 5. FT-IR spectra of Tin sulfide-based nanocomposites.

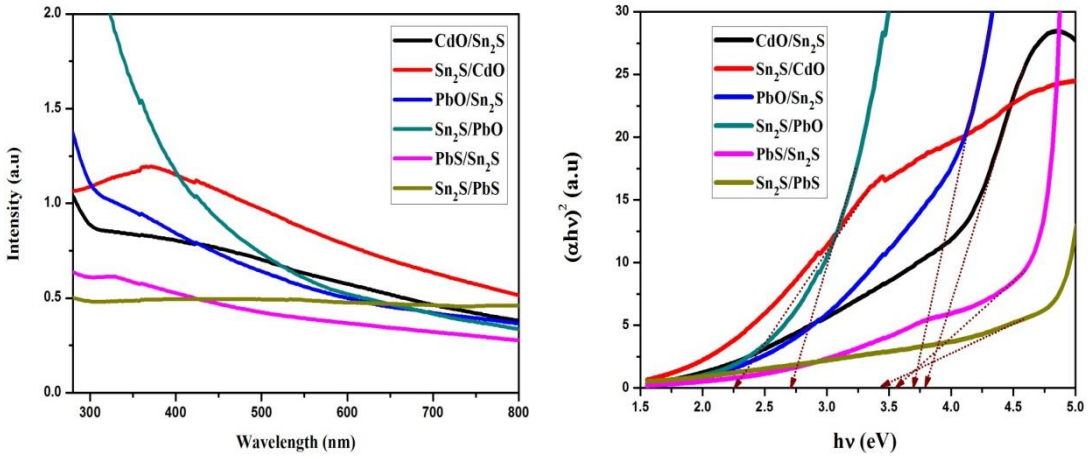

Fig. 6. (a) UV–Vis spectrum of Tin sulfide-based nanocomposites (b) Tauc plot of the nanocomposites for determination of the band gap.

In order to further investigate optical properties, photoluminescence (PL) was performed. Figure 7 shows the room temperature PL spectra of SnS/CdO, CdO/SnS, SnS/PbO, PbO/SnS, SnS/PbS and PbS/SnS nanocomposites. The nanocomposites are clearly showed two distinct emission peaks between 500-550 nm and 550-650 nm range, respectively. All the samples showed green emission at 535, 535, 510, 522, 545 and 524 nm for SnS/CdO, CdO/SnS, SnS/PbO, PbO/SnS, SnS/PbS and PbS/SnS nanocomposites, respectively, it can be originated from Sn vacancies, Sn interstitials, and S vacancies [21]. This green emission in nanocomposites arises due to the number of free electrons and crystal defects. The strong broad emission 550-650 nm observed in CdO/SnS is related to deep energy emission of CdO, which it attributes to the defects and oxygen vacancies present within the CdO lattice [22]. Ravikumar et al. reported a similar strong peak at 605 nm arises due to the combination of the electron from the conduction band and hole from the valance band [23]. Similarly, an emission peak (oxygen vacancy) around 600 nm and 630 nm were observed for PbO/SnS. and PbO/SnS nanocomposite. In addition, strong emission peak at 620 nm and 574 nm obtained for SnS/PbS and PbS/SnS nanocomposites, respectively. The emission peak should be in the range of 560 to 630 nm, which conforms to the PbS structure [24].

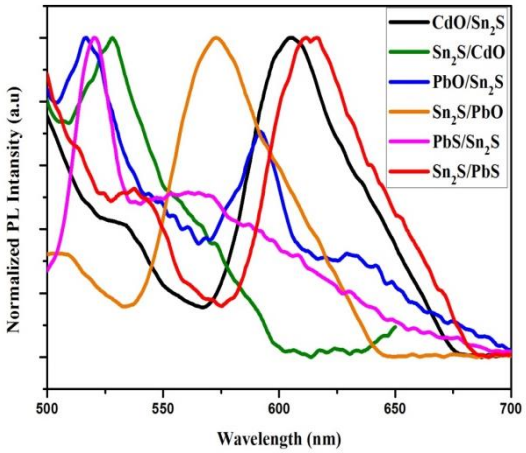

Fig. 7. Photoluminescence spectra of Tin sulfide-based nanocomposites.

4. Conclusions

The various Sn based binary nanocomposites such as SnS/CdO, CdO/SnS, SnS/PbO, PbO/SnS, SnS/PbS and PbS/SnS were prepared by co-precipitation method. Structural, morphological, and optical properties of the as-synthesized nanostructure were studied by XRD, TEM, FT-IR, UV-Vis and PL study. XRD result confirms that the composite is composed of mixed crystal structure of the compounds. These SnS based nanocomposites can be distinctly categorized depending on their size and morphology. This research demonstrates the promising way of synthesis of SnS based binary inorganic nanocomposites for optoelectronic application and it can be extended to photovoltaic application.

Acknowledgements

The author Dr. G. Murugadoss thanks the Chancellor, President, and Vice Chancellor, Sathyabama Institute of Science and Technology, Chennai for the support and encouragement. One of author (Manavalan Rajesh Kumar) thanks to the contract no. 40/is2 and MES of RF (contract no. FEUZ-2020-0051). The authors thank for the financial support by the Researchers Supporting Project Number (**RSP-2021/354**) King Saud University, Riyadh, Saudi Arabia.

References

[1] C. Tan, X. Cao, X.-J. Wu, Q. He, J. Yang, X. Zhang, J. Chen, W. Zhao, S. Han, G.-H. Nam, M. Sindoro, H. Zhang, Chem. Rev. 117, 6225 (2017); https://doi.org/10.1021/acs.chemrev.6b00558

[2] D. Sarkar, X. Xie, W. Liu, W. Cao, J. Kang, Y. Gong, S. Kraemer, P. M. Ajayan, K. Banerjee, Nature 526, 91 (2015); https://doi.org/10.1038/nature15387

[3] A. Pospischil, M. M. Furchi, T. Mueller, Nat. Nanotech. 9, 257 (2014); https://doi.org/10.1038/nnano.2014.14

[4] B. Radisavljevic, A. Radenovic, J. Brivio, V. Giacometti, A. Kis, Nat. Nanotech. 6, 147 (2011); https://doi.org/10.1038/nnano.2010.279

[5] C. Huang, S. Wu, A. M. Sanchez, J. J. P. Peters, R. Beanland, J. S. Ross, P. Rivera, W. Yao, D. H. Cobden, X. Xu, Nat. Mater. 13, 1096 (2014); https://doi.org/10.1038/nmat4064

[6] Y. Gong, J. Lin, X. Wang, G. Shi, S. Lei, Z. Lin, X. Zou, G. Ye, R. Vajtai, B. I. Yakobson, H. Terrones, M. Terrones, B. K. Tay, J. Lou, S. T. Pantelides, Z. Liu, W. Zhou, P. M. Ajayan, Nat. Mater. 13, 1135 (2014); https://doi.org/10.1038/nmat4091

[7] S. Lei, X. Wang, B. Li, J. Kang, Y. He, A. George, L. Ge, Y. Gong, P. Dong, Z. Jin, G. Brunetto, W. Chen, Z.-T. Lin, R. Baines, D. S. Galvão, J. Lou, E. Barrera, K. Banerjee, R. Vajtai, P. Ajayan, Nat. Nanotech. 11, 465 (2016); https://doi.org/10.1038/nnano.2015.323

[8] K. F. Mak, C. Lee, J. Hone, J. Shan, T. F. Heinz, Phys. Rev. Lett. 105, 136805 (2010); https://doi.org/10.1103/PhysRevLett.105.136805

[9] D. Mrinmoy, S. G. Partha, M. R. Vincent, Adv. Mater. 20, 4225 (2008); https://doi.org/10.1002/adma.200703183

[10] Y. Wang, Z. Tang, N. A. Kotov, Materials Today 2005, 20, (2005); https://doi.org/10.1016/S1369-7021(05)00892-8

[11] N. Venkatesh, S. Aravindan, K. Ramki, G. Murugadoss, R. Thangamuthu, P. Sakthivel, Environ. Sci. and Pollut. Res. 28, 16792 (2021); https://doi.org/10.1007/s11356-020-11763-3

[12] X. Li, J. Zhu, H. Li, Appl. Catal. B: Environ. 123-124, 174 (2012); https://doi.org/10.1016/j.molcata.2011.12.006

[13] Q. Li, H. Meng, J. G. Yu, Chem. Eur. J. 20, 1176 (2014); https://doi.org/10.1002/chem.201303446

[14] D. Prabha, K. Usharani, S. Ilangovan, M. Suganya, S. Balamurugan, J. Srivind, V. S. Nagarethinam, A.R. Balu, Mater. Tech. 33, 1 (2018); https://doi.org/10.1080/10667857.2018.1444566

[15] A. Tadjarodi, M. Imani, H. Kerdari, Mater. Res. Bull. 48, 935 (2013); https://doi.org/10.1016/j.materresbull.2012.11.042

[16] M. Kanjwal, N. M. Barakat, F. Sheikh, H. Kim, J. Mater. Sci. 45, 1272 (2010); https://doi.org/10.1007/s10853-009-4078-3

[17] G. Murugadoss, R. Jayavel, M. Rajesh Kumar, Superlatt. and Microstruc. 76, 349 (2014); https://doi.org/10.1016/j.spmi.2014.10.027

[18] S. D. Meshram, R. V. Rupnarayan, S. V. Jagtap, V. G. Mete, V. S. Sangawar, Inter. J. Chem. and Phys. Sci. 4, 83 (2015).

[19] S. M. Lee, Y. W. Jun, S. N. Cho, J. W. Cheon, J. Am. Chem. Soc. 124, 11244 (2002); https://doi.org/10.1021/ja026805j

[20] Y. B. Zhao, J. H. Zou, W. F. Shi, J. Mater. Sci. Eng. B 121, 20 (2005); https://doi.org/10.1016/j.mseb.2005.02.051

[21] N. Venkatesh, K. Sabarish, G. Murugadoss, R. Thangamuthu, P. Sakthivel, Environ. Sci. and Pollut. Res. 27, 43212 (2020); https://doi.org/10.1007/s11356-020-10268-3

[22] D. Antosoly, S. Ilangovan, V. S. Nagarethinam, A. R. Balu, Surf. Eng. 33, 835 (2017).

[23] M. Ravikumar, R. Chandramohan, K. Deva Arun, Kumar, S. Valanarasu, V. Ganesh, M. Shkir, S. AlFaify, A. Kathalingam, Bull. Mater. Sci. 42, 8 (2019); https://doi.org/10.1007/s12034-018-1688-x

[24] C. Rajashree, A. R. Balu, V. S. Nagarethinam, J. Mater. Sci. Mater. Electron. 27, 7876 (2016); https://doi.org/10.1007/s10854-016-4778-9